Research Article

JPIS Journal of Periodontal & Implant Science

J Periodontal Implant Sci 2012;42:50-58 • http://dx.doi.org/10.5051/jpis.2012.42.2.50

Periodontal tissue reaction to customized nano-hydroxyapatite block scaffold in one-wall intrabony defect: a histologic study in dogs

Jung-Seok Lee[1,†], Weon-Yeong Park[2,†], Jae-Kook Cha[1], Ui-Won Jung[1], Chang-Sung Kim[1], Yong-Keun Lee[2], Seong-Ho Choi[1,*]

[1]Department of Periodontology, Research Institute for Periodontal Regeneration, Yonsei University College of Dentistry, Seoul, Korea
[2]Department of Dental Biomaterials and Bioengineering, Research Institute of Dental Biomaterials and Bioengineering, Yonsei University College of Dentistry, Seoul, Korea

Purpose: This study evaluated histologically the tissue responses to and the effects of a customized nano-hydroxyapatite (n-HA) block bone graft on periodontal regeneration in a one-wall periodontal-defect model.
Methods: A customized block bone for filling in the standardized periodontal defect was fabricated from prefabricated n-HA powders and a polymeric sponge. Bilateral 4×4×5 mm (buccolingual width×mesiodistal width×depth), one-wall, critical-size intrabony periodontal defects were surgically created at the mandibular second and fourth premolars of five Beagle dogs. In each dog, one defect was filled with block-type HA and the other served as a sham-surgery control. The animals were sacrificed following an 8-week healing interval for clinical and histological evaluations.
Results: Although the sites that received an n-HA block showed minimal bone formation, the n-HA block was maintained within the defect with its original hexahedral shape. In addition, only a limited inflammatory reaction was observed at sites that received an n-HA block, which might have been due to the high stability of the customized block bone.
Conclusions: In the limitation of this study, customized n-HA block could provide a space for periodontal tissue engineering, with minimal inflammation.

Keywords: Bone substitutes, Guided tissue regeneration, Periodontal disease, Tissue engineering, Tissue scaffolds.

INTRODUCTION

The basic concept underlying conventional periodontal regenerative treatment is to provide a space into which neighboring cells can grow [1]. To this end, various bone grafts have been applied to periodontal defects, with or without an occlusive membrane. Almost all of the previous studies have used particulated [2] or moldable [3] types of bone-graft materials for periodontal regeneration, due to the irregularity of periodontal-defect morphology. However, the ideal graft material remains elusive. Caton et al. [4] reported that a particulated bone graft alone in a periodontal defect resulted in a long junctional epithelium rather than periodontal new attachment.

The regeneration of periodontal tissues is rarely achieved because of the biological peculiarities of periodontal defects.

Received: Feb. 8, 2012; **Accepted:** Mar. 14, 2012
***Correspondence:** Seong-Ho Choi
Department of Periodontology, Research Institute for Periodontal Regeneration, Yonsei University College of Dentistry, 50 Yonsei-ro, Seodaemun-gu, Seoul 120-752, Korea
E-mail: shchoi726@yuhs.ac, Tel: +82-2-2228-3189, Fax: +82-2-392-0398
[†]Jung-Seok Lee and Weon-Yeong Park contributed equally to this study.

pISSN 2093-2278
eISSN 2093-2286

First of all, many kinds of resident bacteria can hinder the regenerative process [5,6], and poor initial sealing between the epithelium and the tooth makes it difficult to protect the wound site from the oral environment [1]. Finally, tooth mobility produced by the destruction of the periodontal support can destabilize the periodontal wound healing [7]. In this unstable situation, every bone-graft particle can be subjected to both the macro- and micromovement, so that the early healing process may be halted or be shifted in another direction. Previous studies in which the grafted materials were covered with a membrane to protect their stability found increased periodontal attachment formation [2,8].

Advances in computed tomography (CT) imaging and computer-aided design and manufacturing systems have yielded defect-driven customized block bone fabrication for various bone defects [9-11]. Thus, it is possible to construct and apply a block-type bone-graft material for irregular shape of the periodontal defects. Because of their interconnected skeletal structure, block-type bone-graft material would provide stronger mechanical stability than the particulated type. In addition, wound stability in the early healing phase may increase due to the accurate mechanical fit of the customized bone graft into the defect. However, only a few studies have investigated the use of block-type grafts within a periodontal defect.

The choice of appropriate material for a scaffold is the most important step of the tissue-engineering process, because the properties of the applied material may affect the other critical parameters of tissue engineering [12]. Hydroxyapatite (HA) is one of the most widely used graft biomaterials in both the research and clinical fields [13-15]. HA has a similar composition and structure to natural bone mineral [16], and is known to chemically bond directly to bone when implanted [17,18]. Although these features have led to HA receiving considerable attention as a scaffold for bone tissue engineering, its inconsistent cell reactions-which are dependent upon the surface properties-limit its clinical use in various situations of bone defect [16,19]. To overcome these limitations, a newly developed HA made of nanoparticles was introduced and was reported to exhibit improved protein adsorption capacity [20].

The aim of this study was to determine histologically the tissue responses to and the effects of a customized nano-hydroxyapatite (n-HA) block bone graft on periodontal regeneration, when applied within one-wall periodontal defects established in dogs.

MATERIALS AND METHODS

Animals

This study investigated five male beagle dogs (approximately 15 months old and weighing 9 to 13 kg) that had been bred exclusively for biomedical research purposes. The animal selection and management, surgical protocol, and preparation followed routines approved by the Institutional Animal Care and Use Committee, Yonsei Medical Center, Seoul, Korea.

Materials

Preparation of the nano-HA powder

HA nanoparticles were prepared using the sol-gel process according to previously published methods [21]. In brief, $Ca(NO_3)_2$-$4H_2O$ (99%; Sigma-Aldrich Co., St. Louis, MO, USA) and $(OC_2H_5)_3P$ (97%; Sigma-Aldrich Co.) were used as precursors of the HA sol. The HA sol was prepared by the reaction between the two precursors at a stoichiometric Ca:P ratio of 1.67, and then dried at 950°C.

Preparation of porous n-HA blocks

Porous n-HA blocks were prepared using prefabricated n-HA powders and a polymeric sponge, according to previously published methods [22]. A reticulated polyurethane ester sponge (Regicell, Jehil Urethane Co., Asan, Korea) with dimensions of 7×7×9 mm was used in this experiment. This sponge has 500 three-dimensionally interconnected open pores per linear millimeter. First, n-HA slurry was prepared by dispersing the prepared n-HA powders into distilled water with organic additives such as binder, dispersant, and a drying chemical control additive. The second process was infiltration, in which the porous sponge was immersed into the n-HA slurry several times, followed by being rolling through Teflon twin rollers. The space was controlled to compress and shrink the sponge to 75% of its original thickness. Finally, heat treatment was applied up to 600°C for 2 hours in a Kanthal furnace in order to burn out the sponge entirely and to volatize the organic additives. The remaining HA was then sintered for 2 hours at various temperatures from 650 to 850°C. This entire procedure listed above was repeated twice to thicken the framework of the porous blocks. The finished blocks were trimmed to dimensions of 4×4×5 mm (so that they precisely fitted the periodontal defects) using a low-speed saw (Isomet, Buehler, Lake Bluff, IL, USA).

Surgical protocol

The surgical procedures, extractions, and experimental protocol were performed under general anesthesia induced with intravenous atropine (0.04 mg/kg; Kwangmyung Pharmaceutical, Seoul, Korea) and an intramuscular injection of a combination of xylazine (Rompun, Bayer Korea Ltd, Seoul, Korea) and ketamine (Ketara, Yuhan, Seoul, Korea), followed by inhalation anesthesia (Gerolan, JW Pharmaceutical, Seoul, Korea).

JPIS Journal of Periodontal & Implant Science

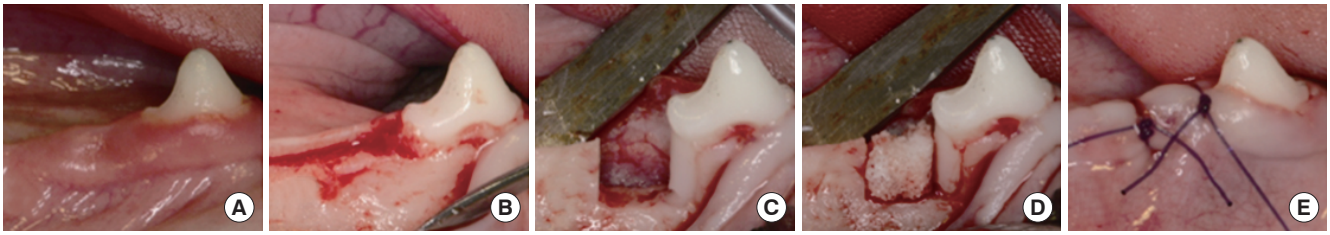

Figure 1. Representative photomicrographs of surgical procedures. (A) Preoperative view, (B) flap elevation, (C) defect creation at the mesial side of the mandibular fourth premolar teeth, (D) application of customized nano-hydroxyapatite block within the defect, and (E) suture with coronally positioned flap.

Routine dental infiltration anesthesia was used at the surgical sites.

An experienced surgeon performed all of the surgeries. First, the mandibular first and third premolars were surgically extracted prior to the experimental surgery. Experimental surgeries were performed following the 8-week healing interval (Fig. 1). Buccal and lingual mucoperiosteal flaps were elevated to create bilateral, critical-size (4×4×5 mm, buccolingual width×mesiodistal width×depth), one-wall intrabony defects at the mesial aspect of the fourth mandibular premolar teeth [23]. Following root planing to remove the root cementum, a reference notch was made into the root surface at the base of each defect. Unilateral defect sites received a customized HA block, which just fitted the site to the level of the alveolar crest. Contralateral sites served as sham-surgery controls. The mucogingival flaps were then advanced, adapted, and sutured for primary-intention healing using horizontal and vertical mattress sutures (Monosyn 4/0, B. Braun Aesculap AG & Co KG, Tuttlingen, Germany). The animals were euthanized at 8 weeks after experiment using intravenous pentobarbital sodium (90 to 120 mg/kg). Block sections including the defect sites and the surrounding alveolar bone and mucosal tissues were collected.

Radiographic analysis using micro-CT images

Block sections were dissected and fixed in 10% neutral buffered formalin for 10 days. The fixed specimens were scanned using micro-CT (μCT; SkyScan 1072, SkyScan, Aartselaar, Belgium) at a resolution of 35 μm (100 kV and 100 μA). The scanned data were converted into digital imaging and communications in medicine format and the experimental area was reconstructed using On Demand 3D software (CyberMed Inc., Seoul, Korea). The overall topography of the defect sites with or without the HA graft was visualized in a three-dimensionally reconstructed image, which allowed the total grafted volume to be calculated.

Histological processing

The block specimens were rinsed in sterile saline and immersed in 10% neutral buffered formalin at a volume 10 times that of the block section for 10 days. Once rinsed in sterile water, the sections were decalcified in 5% formic acid for 14 days, trimmed, dehydrated in a graded ethanol series, and embedded in paraffin. Step-serial sections, 5-μm thick, were cut in a mesial-distal vertical plane at approximately 80-μm intervals. One of the most central sections was stained with hematoxylin and eosin, and the other section was stained with Masson's trichrome.

Histologic and histometric analysis

One experienced masked examiner performed the histologic/histometric analysis using incandescent- and polarized-light microscopy (Research System Microscope BX51, Olympus Co., Tokyo, Japan) and a PC-based image-analysis system (Image-Pro Plus, Media Cybernetics Inc., Silver Spring, MD, USA). The following linear measurements were made at a magnification of ×40:

1) *Defect height*: distance from the notch to the cementoenamel junction (CEJ); 2) *Epithelial attachment:* distance from CEJ to the apical extension of an epithelial attachment on the root surface; 3) *Connective-tissue attachment*: distance from the apical extension of the junctional epithelium to the coronal extension of cementum formation; 4) *Cementum regeneration*: distance from the base of the apical extension of root planing to the coronal extension of newly formed cementum or a cementum-like substance on the root surface; 5) *Bone regeneration*: distance from the base of the apical extension of root planing to the coronal extension of newly formed bone along the root surface; and 6) *Mineralized tissue*: distance from the base of the apical extension of root planing to the coronal extension of the mineralized tissue (residual n-HA block).

Statistical analysis

Summary statistics (mean±standard deviation values) based on animal means for the experimental treatments were calculated using the three central sections from each defect, with defects being averaged for each site. Unpaired *t*-test was used to compare control and experimental groups, with

the level of statistical significance set at 5%.

RESULTS

Clinical and radiographic observations

All defect sites healed uneventfully with minimal signs of inflammation, except for one control site exhibiting gingival recession.

The radiographic evaluation revealed the formation of radiopaque mineralized tissue, with this being greater for sites that received an n-HA block than in the sham-surgery control. The appearance of mineralized tissue at a defect site differed from that of natural bone tissue, with aggregated small particles in contact with the native bone and the denuded root surface, and a few particles observed beyond the graft area (Fig. 2).

Histologic observations

The HA block occupied all the spaces of the periodontal defect in all of the experimental sites, but there was minimal new bone formation around the grafted biomaterials (Fig. 3). Control sites at the base of the defect showed slight bone formation along the root surface, whereas sites that received an n-HA block showed minimal bone formation into the grafted area. Almost all of the residual n-HA biomaterials were localized within the defect site, contacting the neighboring bone and the tooth via a layer of connective tissue. The upper surface of the HA block was covered with periosteum-like connective tissue, with no infiltration by inflammatory cells.

Multinuclear osteoclast-like cells were observed on the surface of almost all residual HA particles (Fig. 4), indicating ongoing biodegradation. There were minimal infiltrations of

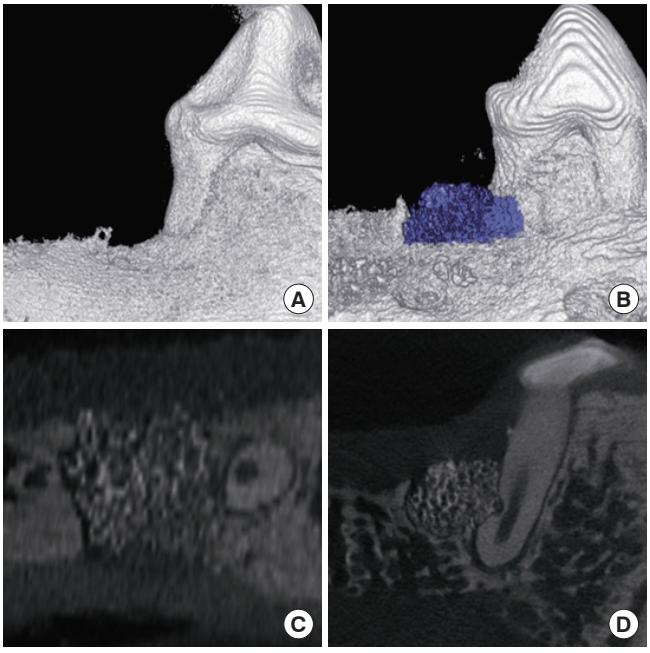

Figure 2. Representative micro computed tomography images of control and experimental site at 8 weeks after surgery. Three-dimensional reconstruction of (A) the control and (B) the experimental site. The part highlighted in blue is the residual nano-hydroxyapatite (n-HA) block (left). (C) Transverse and (D) sagittal cross-sections of the experimental site reveals a well-maintained n-HA block within the defect.

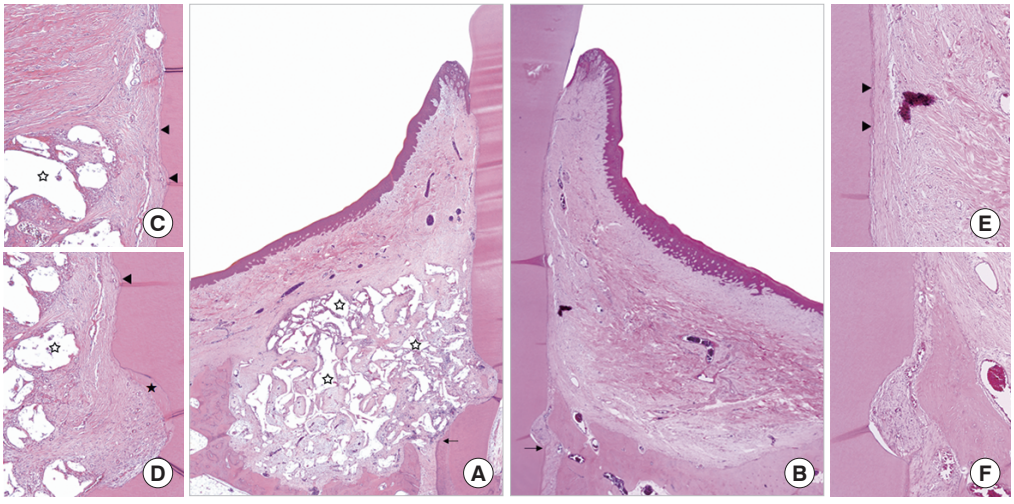

Figure 3. Representative photomicrographs (Hematoxylin and eosin staining) from control (B, E, and F) and experimental sites (A, C, and D). A low-magnification view of the experimental site (A, ×40) shows well-maintained biomaterial (white asterisk) within the defect with connective-tissue ingrowth and minimal bone formation, whereas control site (B, ×40) shows slight linear bone growth and the collapse of soft tissues into the defect site. In the high magnification photomicrographs (C to F, ×100), thick cellular cementum (black asterisk) is observed at the notch area, and thin acellular cementum formation in the area remote from the base of the defect (arrow).

JPIS Journal of Periodontal & Implant Science

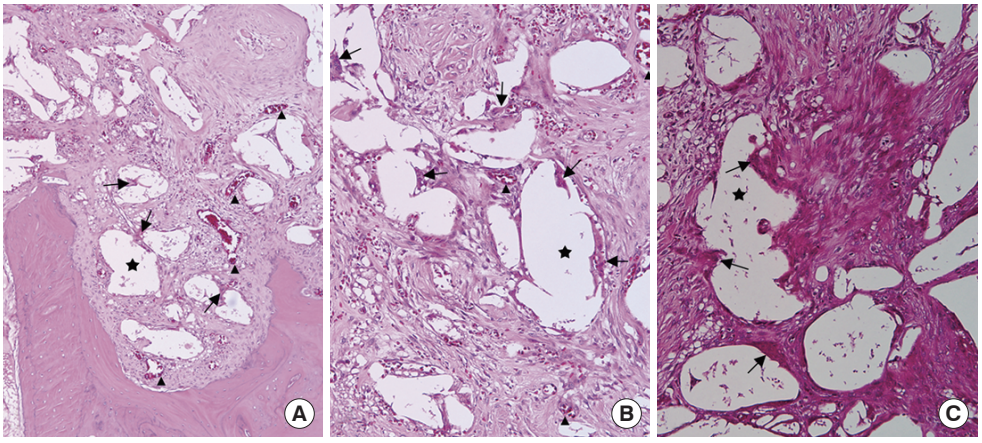

Figure 4. High magnification photomicrographs (Hematoxylin and eosin staining, ×200) from the sites received nano-hydroxyapatite (n-HA) block. (A) Surface resorption with subsiding of n-HA biomaterials into the native bone is observed at the base of the defect, in which n-HA block contacting to the native bone. (B, C) Space within the n-HA block is filled with connective tissues comprised of collagen fibers, fibroblasts, newly formed blood vessels (arrowhead), and osteoclast-like multinuclear cells onto the residual biomaterials (arrow). In some area (C), dense collagen fibers and extensive fibroblasts arranged in a same direction are observed between the residual n-HA biomaterials.

Table 1. Results of radiographic and histometric analysis

	Sham-surgery	n-HA
Radiographic measurements (mm)		
Defect height	6.02±0.57	5.43±0.31
Bone regeneration	0.85±0.67	2.27±0.38
Histologic measurements (mm)		
Defect height	5.48±0.70	5.05±0.61
Epithelial attachment	1.40±0.66	1.22±0.40
Connective tissue attachment	1.61±1.33	0.87±0.62
Cementum regeneration	2.46±0.81	2.75±0.38
Bone regeneration	1.31±1.15	0.86±0.67
Mineralized tissue		2.26±0.26

Values are presented as mean±SD.
n-HA: nano-hydroxyapatite.

inflammatory cells into the spaces around or within the grafted n-HA block. Most of the spaces within n-HA block grafts were filled with a loose connective-tissue matrix that contained large numbers of fibroblasts and a loose collagen fiber network. In addition, numerous newly formed vessels were observed around the particles. However, in some areas there were dense collagen fibers and fibroblasts arranged perpendicular to the surface of the HA particles.

Newly formed cementum with inserting collagen fibrils was observed on the denuded root surface at all of the experimental and control sites (Fig. 3). A thick, cellular, mixed-fiber, stratified cementum (CMSC) appeared to be contiguous with the native cementum at the base of the defect. Functionally oriented collagen fibers ran in a perpendicular direction and inserted into the outer surface of the newly formed cementum. In these area of experimental sites, collagen fibers originating from the space between the HA particles passed and were inserted perpendicularly or obliquely. However, newly formed cementum remote from the base of the defect constituted a thin and acellular extrinsic fiber cementum, with collagen fibers that were arranged obliquely and attached to the new cementum. The observed structures of the new attachments in this area did not differ significantly between the experimental and control specimens.

Histometric analysis and radiographic measurements on μCT

The results of the measurements are given in Table 1. μCT measurements revealed that the amount of bone regeneration was 0.85±0.67 and 2.27±0.38 mm in the control and experimental groups, respectively. Radiographic analysis revealed that the bone regeneration was significantly greater in the HA block group than in the control group.

Histometric analysis revealed that the epithelial attachment was 1.40±0.66 and 1.22±0.40 mm in control and experimental groups, respectively; the corresponding values for nonspecific connective-tissue adhesion were 1.61±1.33 and 0.87±0.62 mm. Cementum regeneration was 2.46±0.81 and 2.75±0.38 mm in control and experimental groups, respectively, while bone regeneration was 1.31±1.15 and 0.86±0.67 mm. Mineralized tissue in experimental sites was measured linearly: 2.26±0.26 mm from the base of the defect. None of the histometric parameters measured differed significantly between the two groups.

DISCUSSION

The aim of the present study was to evaluate a customized

n-HA block graft as a scaffold for periodontal regeneration in the well-established one-wall periodontal defect model in beagle dogs. Limited new bone formation was observed within the defect sites that received an n-HA block, whereas sites that received sham control surgery showed slight bone regeneration (Fig. 3), which was consistent with previous studies that employed this one-wall defect model showing new bone filling linearly up to the apical quarter of the defect that received sham surgery [23,24]. The present result showed significantly increased bone regeneration in radiographic observations, however, limited bone regeneration could be found histologically. This might be caused by the radiopacity of the residual HA block, in spite of the minimal bone formation.

The minimal bone formation at the experimental sites can be attributed to two factors: absence of a barrier membrane and the slow biodegradation process of an n-HA block. Previous studies found significantly more periodontal regeneration within the space protected by a barrier membrane than in the defects without a membrane, regardless of the bone graft materials [25,26]. However, the present study was designed to focus on the maintenance of space and the biocompatibility as a scaffold for periodontal regeneration, and hence a membrane was not used as a barrier. While exclusionary features are known to be the most important requirements of the scaffold for making a protected space [1], recent studies have tried using self-creating cells rather than relying neighboring cells to grow into the protected space [27]. Therefore, self-space maintenance and biocompatibility for cell attachment should be emphasized over the exclusionary features.

Our previous evaluation of tricalcium phosphate particle grafts using the same model identified extensive bone formation in areas with intact native tissues, despite there being no protection from a barrier membrane [24]. However, these areas showed little bone formation in the present study, with instead surface-bone resorption of the native tissue contacting biomaterials being evident (Fig. 4). Such observations might result from the different biodegradation patterns of particulated and block-type biomaterials. Some previous studies [28,29] found less biodegradation and bone formation with block bone grafts in lateral or calvarial defects. In calvarial defects that received particulated bone, new bone formation occurred on the surface of individual particles of biomaterials, and grew into the spaces between them over a longer healing period. However, less bone formation was observed at sites that received a block bone graft, starting from the surface of the grafted block bone and growing into the deeper area over a longer healing period [28].

Despite limited bone formation, the specimens in the experimental groups showed osteoclast-like multinuclear cells and newly formed vessels above and around the residual biomaterials (Fig. 4). These could represent an ongoing process of biodegradation, and alveolar bone formation could be expected within the graft site during a long-term observation period. However, the slow rate of the biodegradation process can prolong the period during which the newly formed tissues are too weak to resist periodontal pathogens. This has prompted many investigations into how to facilitate the regenerative potential [24,30,31]. Recent studies found that bone formation occurred from the core of HA blocks that were used in combination with cell transplantation directly into the block graft [21,32]. In addition, many growth factors reportedly enhance bone regeneration within block-type biomaterials [28,29,33].

Our grafted n-HA block remained almost unchanged within the defect, even though there was some shrinkage and surface remodeling. A grafted block with a hexahedral shape was observed radiographically and histologically (Figs. 2 and 3), whereas top of the residual biomaterials placed more apically than the initial height at the surgery (Figs. 1 and 2). There were no residual particles beyond the hexahedral shape of the graft site, especially in the area of supra-alveolar connective tissue (Fig. 3). This differs from the results of a previous study using particulated bone graft for a periodontal regeneration, in which the scattered residual biomaterials that were observed within the connective tissue area appeared to be associated with extension of the junctional epithelium [24]. Although there was extensive alveolar bone formation in that study, the epithelial attachment extended significantly more apically, and the level of cementum formation was lower at sites that received a particulated bone graft than at the sham-surgery control sites [24]. These differences between the studies could be attributable to the mechanical stability of the block bone graft alone, and its mechanical fitness into the defect.

In a contained defect, a graft with particulated biomaterial can show successful bone regeneration [34,35]. However, an uncontained defect cannot provide sufficient stability to the graft during the initial healing process. This can result in particulated biomaterials being scattered beyond the defect site during the postoperative swelling, with a foreign-body reaction possibly being induced around the biomaterials [36,37]. One of the reasons for using a barrier membrane in a periodontal defect is to provide stability of the blood clot and grafted materials [38,39]. In the present study we found that although the biodegradation process was retarded, sites that received an n-HA block showed aggregated biomaterials only within the defect, minimal inflammation, and limited apical extension of the epithelium (Fig. 3A). Remarkably, new attachments formed between the maintained HA block and the denuded root surface. At the base of the defect, the new

JPIS Journal of Periodontal & Implant Science

attachment included a thick CMSC and many fibers inserting into the newly formed cementum (Fig. 3D). However, the cementum gradually thinned at the upper area of the defect (Fig. 3C), comprised of mainly phase I/II (the early healing phase of Araujo's classification) cementum regeneration [40]. In addition, collagen fibers originating from the pore space of the grafted HA block ran into the newly formed cementum perpendicularly (Fig. 3D).

Bartold et al. [1] suggested that wound stability and functional epithelial sealing in the early healing phase of periodontal regeneration affect the regenerative potential. However, many recent studies have found that grafted biomaterials delay the normal healing process. Because the block-type graft used in the present study was localized within the defect site, and separated from the upper side of the connective and epithelial tissues (Fig. 3A), the presence of unhampered healing in the connective tissue and epithelium might have affected the new attachments formation at the experimental site.

In conclusion, the present study evaluated histologically the tissue responses to and the effects of a customized n-HA block bone graft on periodontal regeneration in a one-wall periodontal-defect model. Within the limitations of this study, the customized n-HA block was maintained with the original hexahedral shape within the defect site, and its stability in the defect might have been responsible for the minimal inflammation observed in the periodontal defects. Although these appear to be clear advantages of using a customized n-HA block as a scaffold for periodontal regeneration, further studies are needed to improve both the biodegradation and the alveolar bone tissue regeneration.

CONFLICT OF INTEREST

No potential conflict of interest relevant to this article was reported.

ACKNOWLEDGEMENTS

This study was supported by a grant of the Korea Health Technology R&D Projects, Ministry of Health & Welfare, Republic of Korea (101578).

REFERENCES

1. Bartold PM, McCulloch CA, Narayanan AS, Pitaru S. Tissue engineering: a new paradigm for periodontal regeneration based on molecular and cell biology. Periodontol 2000 2000;24:253-69.
2. Trombelli L. Which reconstructive procedures are effective for treating the periodontal intraosseous defect? Periodontol 2000 2005;37:88-105.
3. Bender SA, Rogalski JB, Mills MP, Arnold RM, Cochran DL, Mellonig JT. Evaluation of demineralized bone matrix paste and putty in periodontal intraosseous defects. J Periodontol 2005;76:768-77.
4. Caton J, Nyman S, Zander H. Histometric evaluation of periodontal surgery. II. Connective tissue attachment levels after four regenerative procedures. J Clin Periodontol 1980;7:224-31.
5. Heitz-Mayfield L, Tonetti MS, Cortellini P, Lang NP; European Research Group on Periodontology (ERGOPERIO). Microbial colonization patterns predict the outcomes of surgical treatment of intrabony defects. J Clin Periodontol 2006;33:62-8.
6. Machtei EE, Cho MI, Dunford R, Norderyd J, Zambon JJ, Genco RJ. Clinical, microbiological, and histological factors which influence the success of regenerative periodontal therapy. J Periodontol 1994;65:154-61.
7. Schulz A, Hilgers RD, Niedermeier W. The effect of splinting of teeth in combination with reconstructive periodontal surgery in humans. Clin Oral Investig 2000;4:98-105.
8. Needleman IG, Worthington HV, Giedrys-Leeper E, Tucker RJ. Guided tissue regeneration for periodontal infra-bony defects. Cochrane Database Syst Rev 2006;(2):CD001724.
9. Ciocca L, De Crescenzio F, Fantini M, Scotti R. CAD/CAM and rapid prototyped scaffold construction for bone regenerative medicine and surgical transfer of virtual planning: a pilot study. Comput Med Imaging Graph 2009;33:58-62.
10. Dellinger JG, Cesarano J 3rd, Jamison RD. Robotic deposition of model hydroxyapatite scaffolds with multiple architectures and multiscale porosity for bone tissue engineering. J Biomed Mater Res A 2007;82:383-94.
11. Sun W, Darling A, Starly B, Nam J. Computer-aided tissue engineering: overview, scope and challenges. Biotechnol Appl Biochem 2004;39(Pt 1):29-47.
12. Hutmacher DW. Scaffolds in tissue engineering bone and cartilage. Biomaterials 2000;21:2529-43.
13. Benlidayi ME, Kurkcu M, Oz IA, Sertdemir Y. Comparison of two different forms of bovine-derived hydroxyapatite in sinus augmentation and simultaneous implant placement: an experimental study. Int J Oral Maxillofac Implants 2009;24:704-11.
14. De Santis E, Botticelli D, Pantani F, Pereira FP, Beolchini M, Lang NP. Bone regeneration at implants placed into extraction sockets of maxillary incisors in dogs. Clin Oral Implants Res 2011;22:430-7.
15. Jensen T, Schou S, Stavropoulos A, Terheyden H, Holmstrup P. Maxillary sinus floor augmentation with Bio-Oss or Bio-Oss mixed with autogenous bone as graft: a sys-

tematic review. Clin Oral Implants Res 2012;23:263-73.
16. Wang H, Li Y, Zuo Y, Li J, Ma S, Cheng L. Biocompatibility and osteogenesis of biomimetic nano-hydroxyapatite/polyamide composite scaffolds for bone tissue engineering. Biomaterials 2007;28:3338-48.
17. de Bruijn JD, van Blitterswijk CA, Davies JE. Initial bone matrix formation at the hydroxyapatite interface in vivo. J Biomed Mater Res 1995;29:89-99.
18. Okumura M, Ohgushi H, Dohi Y, Katuda T, Tamai S, Koerten HK, et al. Osteoblastic phenotype expression on the surface of hydroxyapatite ceramics. J Biomed Mater Res 1997;37:122-9.
19. Deligianni DD, Katsala ND, Koutsoukos PG, Missirlis YF. Effect of surface roughness of hydroxyapatite on human bone marrow cell adhesion, proliferation, differentiation and detachment strength. Biomaterials 2001;22:87-96.
20. Wei G, Ma PX. Structure and properties of nano-hydroxyapatite/polymer composite scaffolds for bone tissue engineering. Biomaterials 2004;25:4749-57.
21. Jang YJ, Jung IH, Park JC, Jung UW, Kim CS, Lee YK, et al. Effect of seeding using an avidin-biotin binding system on the attachment of periodontal ligament fibroblasts to nanohydroxyapatite scaffolds: three-dimensional culture. J Periodontal Implant Sci 2011;41:73-8.
22. Park YS, Kim KN, Kim KM, Choi SH, Kim CK, Legeros RZ, et al. Feasibility of three-dimensional macroporous scaffold using calcium phosphate glass and polyurethane sponge. J Mater Sci 2006;41:4357-64.
23. Kim CS, Choi SH, Chai JK, Cho KS, Moon IS, Wikesjo UM, et al. Periodontal repair in surgically created intrabony defects in dogs: influence of the number of bone walls on healing response. J Periodontol 2004;75:229-35.
24. Lee JS, Wikesjo UM, Jung UW, Choi SH, Pippig S, Siedler M, et al. Periodontal wound healing/regeneration following implantation of recombinant human growth/differentiation factor-5 in a beta-tricalcium phosphate carrier into one-wall intrabony defects in dogs. J Clin Periodontol 2010;37:382-9.
25. Cortellini P, Tonetti MS. Clinical performance of a regenerative strategy for intrabony defects: scientific evidence and clinical experience. J Periodontol 2005;76:341-50.
26. Tonetti MS, Cortellini P, Lang NP, Suvan JE, Adriaens P, Dubravec D, et al. Clinical outcomes following treatment of human intrabony defects with GTR/bone replacement material or access flap alone. A multicenter randomized controlled clinical trial. J Clin Periodontol 2004;31:770-6.
27. Urciuolo F, Imparato G, Guaccio A, Mele B, Netti PA. Novel strategies to engineering biological tissue in vitro. Methods Mol Biol 2012;811:223-44.
28. Kim JW, Choi KH, Yun JH, Jung UW, Kim CS, Choi SH, et al. Bone formation of block and particulated biphasic calcium phosphate lyophilized with Escherichia coli-derived recombinant human bone morphogenetic protein 2 in rat calvarial defects. Oral Surg Oral Med Oral Pathol Oral Radiol Endod 2011;112:298-306.
29. Schwarz F, Rothamel D, Herten M, Ferrari D, Sager M, Becker J. Lateral ridge augmentation using particulated or block bone substitutes biocoated with rhGDF-5 and rhBMP-2: an immunohistochemical study in dogs. Clin Oral Implants Res 2008;19:642-52.
30. Murakami S. Periodontal tissue regeneration by signaling molecule(s): what role does basic fibroblast growth factor (FGF-2) have in periodontal therapy? Periodontol 2000 2011;56:188-208.
31. Wikesjo UM, Sorensen RG, Kinoshita A, Jian Li X, Wozney JM. Periodontal repair in dogs: effect of recombinant human bone morphogenetic protein-12 (rhBMP-12) on regeneration of alveolar bone and periodontal attachment. J Clin Periodontol 2004;31:662-70.
32. Kawase T, Okuda K, Kogami H, Nakayama H, Nagata M, Sato T, et al. Human periosteum-derived cells combined with superporous hydroxyapatite blocks used as an osteogenic bone substitute for periodontal regenerative therapy: an animal implantation study using nude mice. J Periodontol 2010;81:420-7.
33. De Angelis N, Scivetti M. Lateral ridge augmentation using an equine flex bone block infused with recombinant human platelet-derived growth factor BB: a clinical and histologic study. Int J Periodontics Restorative Dent 2011;31:383-8.
34. Araujo M, Linder E, Lindhe J. Effect of a xenograft on early bone formation in extraction sockets: an experimental study in dog. Clin Oral Implants Res 2009;20:1-6.
35. Araujo MG, Liljenberg B, Lindhe J. Dynamics of Bio-Oss Collagen incorporation in fresh extraction wounds: an experimental study in the dog. Clin Oral Implants Res 2010;21:55-64.
36. Carmagnola D, Berglundh T, Araujo M, Albrektsson T, Lindhe J. Bone healing around implants placed in a jaw defect augmented with Bio-Oss. An experimental study in dogs. J Clin Periodontol 2000;27:799-805.
37. Carmagnola D, Berglundh T, Lindhe J. The effect of a fibrin glue on the integration of Bio-Oss with bone tissue. A experimental study in labrador dogs. J Clin Periodontol 2002;29:377-83.
38. Wikesjo UM, Claffey N, Egelberg J. Periodontal repair in dogs. Effect of heparin treatment of the root surface. J Clin Periodontol 1991;18:60-4.
39. Wikesjo UM, Lim WH, Thomson RC, Hardwick WR. Periodontal repair in dogs: gingival tissue occlusion, a critical

JPIS Journal of Periodontal & Implant Science

requirement for GTR? J Clin Periodontol 2003;30:655-64.
40. Araújo MG, Berglundh T, Lindhe J. On the dynamics of periodontal tissue formation in degree III furcation defects. An experimental study in dogs. J Clin Periodontol 1997;24:738-46.